Science of the Total Environment 788 (2021) 147740

Contents lists available at ScienceDirect

Science of the Total Environment

journal homepage: www.elsevier.com/locate/scitotenv

Aggravated ozone pollution in the strong free convection boundary layer

Guiqian Tang [a,b,g], Yuting Liu [a,g], Xiao Huang [c], Yinghong Wang [a,*], Bo Hu [a], Yucui Zhang [d], Tao Song [a], Xiaolan Li [e], Shuang Wu [a], Qihua Li [f], Yanyu Kang [f], Zhenyu Zhu [a], Meng Wang [a], Yiming Wang [a,g], Tingting Li [a], Xin Li [a], Yuesi Wang [a,b,g,**]

[a] State Key Laboratory of Atmospheric Boundary Layer Physics and Atmospheric Chemistry, Institute of Atmospheric Physics, Chinese Academy of Sciences, Beijing 100029, China
[b] Center for Excellence in Urban Atmospheric Environment, Institute of Urban Environment, Chinese Academy of Sciences, Xiamen 361021, China
[c] HuiHua College of Hebei Normal University, Shijiazhuang 050091, China
[d] Key Laboratory of Agricultural Water Resources, Center for Agricultural Resources Research, Institute of Genetics and Developmental Biology, Chinese Academy of Sciences, Shijiazhuang 050021, China
[e] Institute of Atmospheric Environment, China Meteorological Administration, Shenyang, Liaoning 110166, China
[f] Institutes of Physical Science and Information Technology, Anhui University, Hefei 230601, China
[g] University of Chinese Academy of Sciences, Beijing 100049, China

HIGHLIGHTS

- Free and forced convection conditions were classified using remote sensing observations.
- Ozone pollution is related to the intensity of free convection in the boundary layer.
- Ozone-NOx-VOCs sensitivity is closely related to the boundary layer structure.
- The BLH can be used as an indicator to judge ozone pollution under free convection conditions.

GRAPHICAL ABSTRACT

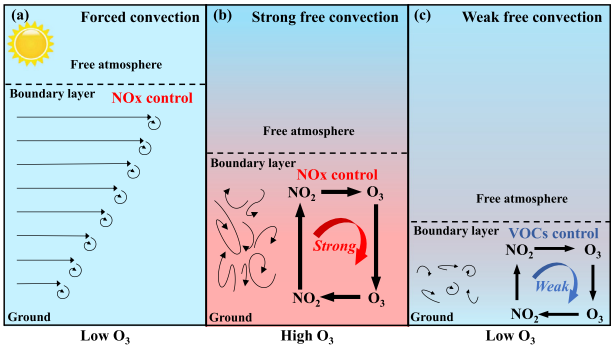

ARTICLE INFO

Article history:
Received 22 February 2021
Received in revised form 5 May 2021
Accepted 9 May 2021
Available online 15 May 2021

Editor: Pingqing Fu

Keywords:
Boundary layer
Forced convection
Free convection
Tethered balloon
Turbulence

ABSTRACT

Clarifying the relationship between meteorological factors and ozone can provide scientific support for ozone pollution prediction, but the effects of boundary layer meteorology, especially boundary layer height and turbulence, on ozone pollution are rarely studied. Here, ozone and its related meteorological factors were observed in summer in Shijiazhuang, a city with the most serious ozone pollution on the North China Plain. The forced and free convection boundary layers were classified using ground remote observations. After eliminating the forced convection condition, strong free convection conditions, exhibiting a high boundary layer height, high wind speed, strong turbulence and large-scale free convection velocity, were found to be beneficial for the aggravation of ozone pollution. Combined with the ozone profile detected by a tethered balloon, the ozone chemical budget was calculated using the differences in the column ozone concentrations between the morning and afternoon, and the results confirmed the impact of free convection intensity on ozone pollution. The change in ozone sensitivity from VOCs sensitivity to NOx sensitivity driven by strong free convection was the main reason for the deterioration of ozone pollution. This study clarified the impact of boundary layer meteorology on ozone and its sensitivity and has important practical significance for ozone pollution prevention and early warning.

* Corresponding author.
** Correspondence to: Y. Wang, State Key Laboratory of Atmospheric Boundary Layer Physics and Atmospheric Chemistry, Institute of Atmospheric Physics, Chinese Academy of Sciences, Beijing 100029, China.
E-mail addresses: wangyinghong@mail.iap.ac.cn (Y. Wang), wys@mail.iap.ac.cn (Y. Wang).

https://doi.org/10.1016/j.scitotenv.2021.147740
0048-9697/

1. Introduction

The main source of tropospheric ozone is not primary emissions but secondary reactions of nitrogen oxides (NOx) and volatile organic compounds (VOCs) under sunlight (Seinfeld and Pandis, 1998). Therefore, the production of tropospheric ozone is controlled by both precursor emissions and meteorological factors. The relationship between ozone and precursors is usually nonlinear and exhibits different evolution characteristics in different regions (Chameides et al., 1992). In North China, as an example, ozone production is usually controlled by VOCs in urban areas but controlled by NOx in remote rural areas (Tang et al., 2012).

Although the emission of ozone precursors is very important, it is very difficult to form ozone without favorable meteorological conditions (Solomon et al., 2000). First, the main pathway of ozone production is the photolysis of nitrogen dioxide (NO_2), and the cycle of free radicals depends on the photolysis of ozone. Both reactions are controlled by solar radiation. Second, hydrogen radicals participate in the reaction during the cycle between nitrogen oxide (NO) and NO_2, which is strictly temperature (T)-dependent (Vukovich, 1994; Jenkin and Clemitshaw, 2000). In addition, water vapor is one of the indispensable conditions for the chemical cycle of free radicals, but a daily average relative humidity (RH) of 40–60% is sufficient (Ellis et al., 2000; Zhao et al., 2019). Strong winds will cause ozone and its precursors to be transported to downwind areas, thus limiting the formation of ozone (Banta et al., 2011; Hidy, 2000). Therefore, strong radiation, high T, moderate RH and calm winds are favorable meteorological conditions for ozone production (Tong et al., 2011).

In addition to the meteorological factors mentioned above, the boundary layer height (BLH) is also a key meteorological parameter for ozone pollution. It is generally believed that a decrease in the BLH will lead to the accumulation of pollutants in the boundary layer, inducing the development of ozone pollution (Banta et al., 1998; Haman et al., 2014). Large-scale studies in Europe also show that stable meteorological conditions are conducive to the occurrence and development of ozone pollution (Garrido-perez et al., 2019). However, previous studies in Philadelphia and Houston, USA, show that a high BLH is a favorable meteorological condition for a high incidence of ozone pollution (Athanassiadis et al., 2002; Rappenglück et al., 2008). Nevertheless, recent studies have shown that the relationship between BLH and ozone concentrations is nonlinear (Banta et al., 2011; Berkowitz et al., 2000). When the BLH is in the range of 1000–1200 m during the daytime, the ozone concentration is usually the highest and then decreases gradually when the BLH exceeds 1200 m (Zhao et al., 2019). Therefore, the impact of boundary layer meteorology on ozone pollution is still uncertain.

The formation and development of the boundary layer mainly depend on turbulence. As is well known, there are two forms of turbulence. One is that the ground is heated by solar shortwave radiation, and then the ground releases longwave radiation to heat the atmosphere. The formation of buoyancy promotes the development of the atmospheric boundary layer. Another is the wind shear caused by a difference in wind speeds (WS) at different heights. A boundary layer dominated by buoyancy is called a free convection boundary layer, while a boundary layer dominated by wind shear is called a forced convection boundary layer (Stull, 1988). Previous studies did not distinguish between the two types of boundary layers, so it is impossible to obtain a clear relationship between boundary layer meteorology and ozone.

Additionally, we usually judge the relationship between ozone concentration and meteorological factors based on the daily maximum ozone concentration in the afternoon (Olszyna et al., 1997). Some studies use the difference between the maximum and minimum ozone concentrations to quantify the amount of ozone production (Tang et al., 2012). However, neither of the two methods can accurately represent the ozone chemical budget. For example, ozone stored in the residual layer during the nighttime can be mixed downward into the ground level with the rise of the BLH during the following day (Zhao et al., 2019; Zhu et al., 2020). The ozone stored in the residual layer is not from chemical production on the same day but remains after formation during the previous day. If we only judge the relationship between ozone concentration and meteorological factors using traditional methods, we cannot eliminate the contribution of vertical downward ozone transport from the residual layer, which will lead to overestimation of ozone production.

From the abovementioned analysis, only by distinguishing the types of atmospheric boundary layers and quantifying the ozone chemical budget during a course of a day is it possible to accurately obtain the response of ozone pollution to boundary layer meteorology. Here, we carried out two field campaigns in Shijiazhuang, which is the area with the most serious photochemical pollution on the North China Plain, and obtained ozone, meteorological and micrometeorological factors simultaneously under different boundary layer conditions. Based on these data and tethered balloon observations, the ozone chemical budget in the boundary layer was calculated, and the relationship between the ozone chemical budget and meteorological factors was analyzed. Finally, the response of ozone to boundary layer meteorology was clarified, and the reasons were discussed.

2. Methodology

The most serious period of ozone pollution on the North China Plain is summer, so two observation campaigns were conducted from August 25 to September 19, 2018 (late summer) and from June 8 to July 2, 2019 (early summer). The observation site is in Shijiazhuang (Fig. S1), which is the city with the most serious photochemical pollution on the North China Plain.

The observation station for meteorological and micrometeorological factors is located in Luancheng district (114° 41′E, 37° 53′N) in southern Shijiazhuang city (Fig. S1). Ultraviolet radiation (UV) was measured by an ultraviolet radiometer (CUV5, Kipp &Zonen, USA), and the detailed measurement principle and data quality control scheme are shown in Hu et al. (2010). T and RH were measured by temperature and humidity sensors (HMP45D, Vaisala, Finland), and WS was measured by a wind speed sensor (WAA15, Vaisala, Finland). A three-dimensional ultrasonic anemometer was used to measure the micrometeorological factors (CSAT3, Campbell Scientific, Inc., USA), and the height for the observation was 3.5 m. Please refer to Zhang et al. (2018) for details of the measurement.

The turbulent kinetic energy (TKE), free convection velocity scale (w^*) and forced convection velocity scale (u^*) were calculated by using the micrometeorological parameters measured by a three-dimensional ultrasonic anemometer to characterize the state of the atmospheric boundary layer (Stull, 1988). The specific calculation method is as follows.

$$\frac{TKE}{m} = \frac{1}{2}\left(\overline{u'^2} + \overline{v'^2} + \overline{w'^2}\right) \tag{1}$$

$$w^* = \left[\frac{gz_i}{\overline{\theta_v}}\left(\overline{w'\theta_v'}\right)\right]^{1/3} \tag{2}$$

$$u^* = \left(\overline{u'w'}^2 + \overline{v'w'}^2\right)^{1/4} \tag{3}$$

where m is the mass, u' is the fluctuating WS in the U direction, v' is the fluctuating WS in the V direction, w' is the fluctuating WS in the W direction, z_i is the BLH, θ_v is the virtual potential temperature and g is the acceleration of gravity.

The observation stations of ground-level ozone, tethered balloon, and BLH measurements are located in Yuanshi County (114° 30′E, 37° 48′N) in southern Shijiazhuang city, only 15 km from the meteorological observation station (Fig. S1). An ozone analyzer (49C, Thermo Fisher Scientific, USA) was used as the ozone monitoring instrument, and a detailed description can be found in Tang et al. (2009) and Text S1 in the

supplementary materials. A tethered balloon was used for the vertical detection of meteorological factors (T, RH, air pressure, WS, and wind direction) from 0 to 1000 m, and the detection results have been well verified in previous studies (Zhao et al., 2019; Wu et al., 2021). The ozone detector was launched with the tethered balloon to measure the ozone concentration with a temporal resolution of 10 s. The selected ozone concentration detection instrument (POM, 2B technology, USA) is based on the ultraviolet absorption principle (Wu et al., 2020), and the observation results are compared well to the traditional electrochemical method (Fig. S2). During the observation period, two groups of samples were collected every day, namely, before sunrise (4:00–6:00 LT) and in the afternoon (13:00–16:00 LT). A total of 46 ozone profiles were obtained, including 22 and 24 profiles in 2018 and 2019, respectively. The real-time atmospheric backscattering coefficient within 0–7.7 km was measured by a ceilometer (CL51, Vaisala, Finland) (Tang et al., 2015). Afterwards, the gradient method was used to calculate the position of the sudden change in the backscattering coefficient to determine the BLH. The specific methods have been reported in detail in previous studies (Tang et al., 2016) and Text S2 in the supplementary materials.

To analyze the response of ozone to boundary layer meteorology, the daily column concentrations of NO_2 and formaldehyde (HCHO) observed by the TROPOspheric Monitoring Instrument (TROPOMI) (37.6–38.1°N, 114.3–114.8°E for Shijiazhuang) were obtained during the observation periods (Zhang et al., 2019). $HCHO/NO_2$ was used as an indicator to illustrate ozone sensitivity under different boundary layer conditions (Tang et al., 2012).

3. Results

3.1. Classification of boundary layer

A total of 51 days of observation data were obtained, including 24 days in 2018 and 27 days in 2019. The detailed time series of ozone and its meteorological factors in the observation periods are shown in the supplementary materials (Figs. S3 and S4). As mentioned above, there are two ways to form turbulence in the boundary layer, namely, buoyancy and wind shear. The formation mechanisms of the two kinds of turbulence are very different. The turbulence formed by buoyancy is from the ground to the upper boundary layer, while the turbulence formed by wind shear may be formed at different atmospheric heights. Therefore, the turbulence formed by buoyancy is terminated when it rises to the top of the boundary layer, which leads to a large difference in the amount of backscattering coefficients inside and outside the boundary layer (Fig. S5a). However, the turbulence formed by wind shear can bring clean air from the free atmosphere into the boundary layer, which makes the difference between the free atmosphere and the boundary layer less obvious (Fig. S5b). Based on this, free and forced convection cannot be classified using near-ground observations. Therefore, the variance in the daytime atmospheric backscattering coefficient within 0–4.5 km is calculated by using the detection results from the ceilometer. The smaller the variance is, the stronger the influence of wind shear is. Weather conditions with a variance in the atmospheric backscattering coefficient less than 0.1 Mm^2/Sr^2 are selected as the forced convection conditions (6 days), and the remaining weather conditions are the free convection conditions (45 days).

Afterwards, the free convection conditions are divided into three levels according to the maximum 8-h moving average ozone ($O_{3\text{-}8M}$): < 40 ppbv (7 days), 40–80 ppbv (13 days) and > 80 ppbv (25 days). The three levels correspond to low ozone pollution (LO_3), moderate ozone pollution (MO_3) and high ozone pollution (HO_3).

3.2. The response of ozone to boundary layer meteorology

The diurnal cycles of ozone and meteorological factors were obtained under the above four types of environmental conditions (Fig. 1). Under free convection conditions, with the rapid increases in UV and T, the ozone concentration increased significantly. Under HO_3 conditions, UV is 2.5 times that of LO_3, T increases by 42%, and the RH decreases by 37%. However, it is also found that strong convection leads to a significant increase in WS and BLH. The WS of HO_3 is 2.2 times that of LO_3, and the BLH is 2.1 times that of LO_3. Under forced convection conditions, UV is the highest, and the maximum value can reach 44.2 W/m^2. T is also very high, with the highest T exceeding 31.4 °C. However, the RH is the lowest, with a minimum of 26.0%. The WS and BLH are also the highest, with a maximum WS greater than 5 m/s and a maximum BLH greater

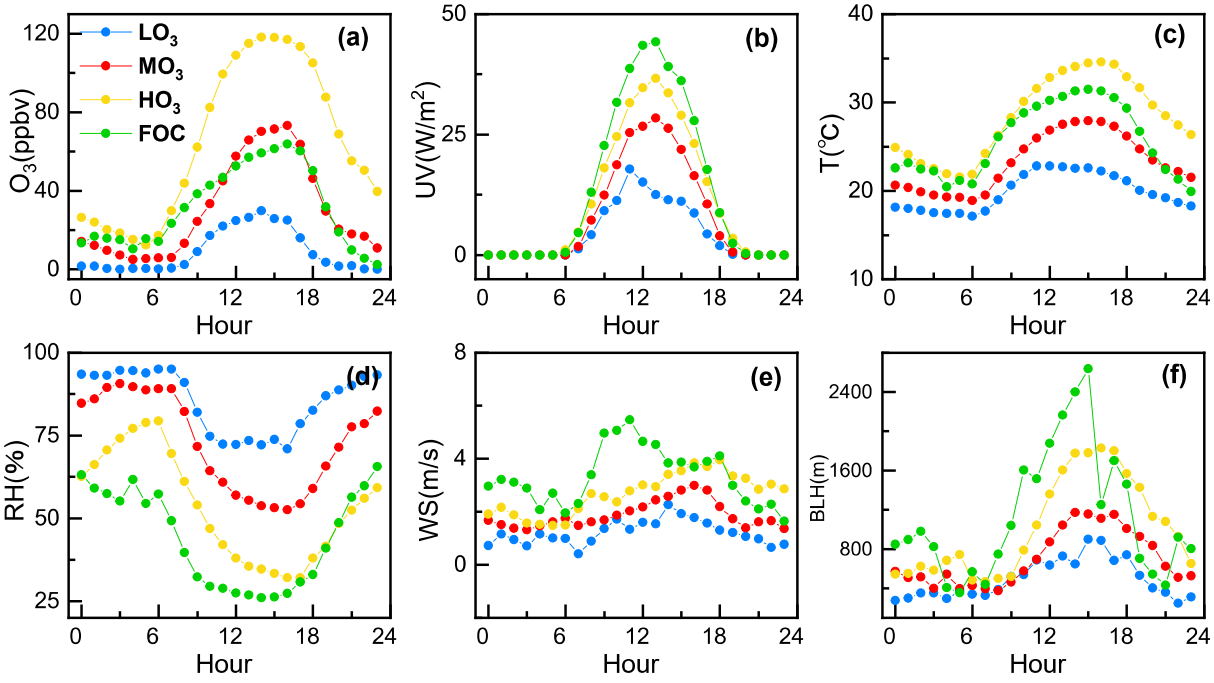

Fig. 1. Diurnal cycles of O_3 (a), UV (b), T (c), RH (d), WS (e) and BLH (f) under different environmental conditions. LO_3, MO_3, and HO_3 denote free convection days with $O_{3\text{-}8M}$ concentrations lower than 40 ppbv, 40–80 ppbv and greater than 80 ppbv, respectively, and FOC denotes forced convection days.

than 2600 m, respectively. Therefore, although UV and T are suitable for ozone production under forced convection conditions, the ozone concentration is not high due to the extremely high WS and BLH, which quickly dilute ozone and its precursors to the downwind areas. Under this condition, $O_{3\text{-}8M}$ is only approximately 50–60 ppbv, which is close to the background ozone concentration.

Through the above analysis, it can be found that the BLH cannot be directly used as a diagnostic indicator of ozone pollution. However, after eliminating the forced convection condition, the BLH can be a good indicator of ozone pollution. In other words, under the conditions of free convection, the stronger the UV, the higher the T, the lower the RH, the higher the WS and the higher the BLH, the more serious the ozone pollution is. This result is significantly different from the previous conclusion that ozone pollution is caused by stable conditions and calm winds (Haman et al., 2014), indicating that the intensity of free convection in the atmospheric boundary layer is positively correlated with the occurrence and development of ozone pollution.

3.3. Evidence of micrometeorology

The above conclusions are obtained from the perspective of meteorological parameters and lack verification of micrometeorological parameters. To verify the importance of free convection intensity to ozone pollution, the same analysis was carried out using the measured micrometeorological parameters (Fig. 2). The results show that the TKE is the highest in the forced convection condition, and the maximum is close to 1.7 m^2/s^2. Except under forced convection, the ozone concentration is positively correlated with TKE. The maximum TKE is 1.1 m^2/s^2 on HO_3 days, while this value is only 0.4 m^2/s^2 on LO_3 days. As TKE is affected by buoyancy and wind shear, it is difficult to distinguish whether the ozone concentration is driven by buoyancy or wind shear based only on the analysis of TKE. To separate these two factors, the velocity scales of free convection and forced convection were calculated (Stull, 1988). Interestingly, except for the highest scale of forced convection velocity (daily mean≈0.3 m/s), the scales of forced convection velocity under LO_3, MO_3 and HO_3 conditions are similar (<0.2 m/s). This provides an excellent situation for analyzing the response of ozone pollution to the free convection intensity. Under the HO_3 conditions, the daily maximum scale of the free convection velocity can even reach 2.0 m/s. Under LO_3 conditions, the scale of the free convection velocity is only 1.2 m/s. In other words, the scale of the free convection velocity is positively correlated with the ozone concentration. Therefore, the evolution of micrometeorological parameters also confirmed that the stronger the free convection was, the higher the ozone concentration was.

3.4. Dominant role of free convection in the ozone chemical budget

Although the above conclusions are rather clear, there is still a loophole. All of the above results are based on ozone concentration and meteorological factors, but the ozone concentration and ozone chemical budget are not the same.

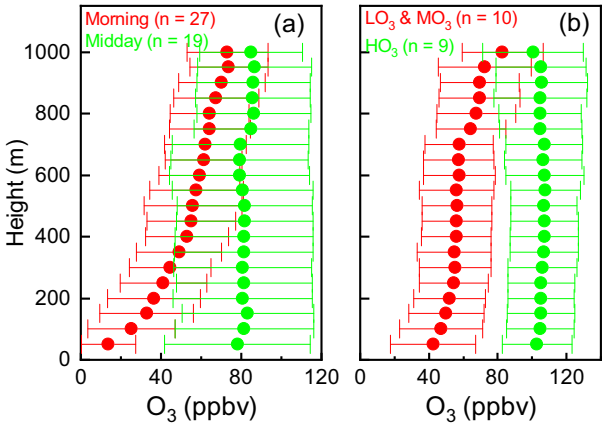

Fig. 3. Averaged vertical ozone profiles in the morning and afternoon during two observation campaigns (a) and under the LO_3, MO_3 and HO_3 conditions at noon (b). LO_3, MO_3, and HO_3 denote free convection days with $O_{3\text{-}8M}$ concentrations lower than 40 ppbv, 40–80 ppbv and greater than 80 ppbv, respectively.

Fig. 1f shows that the BLH presents obvious diurnal variation. During the nighttime, the stable boundary layer is shallow and is close to the ground, and the residual layer is above the stable boundary layer. In the early morning, the ozone concentration in the near-surface layer was affected by the titration of newly emitted NO, and the concentration was very low (< 20 ppbv). However, NOx emissions near the ground have difficulty penetrating the stable boundary layer into the residual layer, resulting in ozone remaining in the residual layer with an average concentration of approximately 60 ppbv (Fig. 3a). Therefore, this typical boundary layer evolution leads to ozone concentrations that are lower in the lower boundary layer and higher in the upper boundary layer in the morning (Tang et al., 2021a). Although the ozone concentrations in the stable boundary layer and the residual layer are quite different in the morning, the ozone concentrations in the boundary layer are relatively uniform in the afternoon (Fig. 3a). The enhancement of radiation in the daytime leads to strong convection and the rise of the boundary layer, which induces the ozone stored in the residual layer to mix downward to the boundary layer, affecting the near-surface ozone concentration (Athanassiadis et al., 2002; Zhao et al., 2019). Therefore, this phenomenon will lead to overestimation of ozone production ability.

To eliminate the impact of residual layer downward mixing, the ozone profiles ($n = 13$, Table S1) observed in the morning and afternoon on the same days were used to calculate the ozone chemical budget (including chemical production and loss) using the difference between the average ozone column concentrations in the boundary layer in the morning and afternoon (Zhao et al., 2019). The results showed that the average column concentration of ozone was 23.1–100.7 ppbv in the morning and

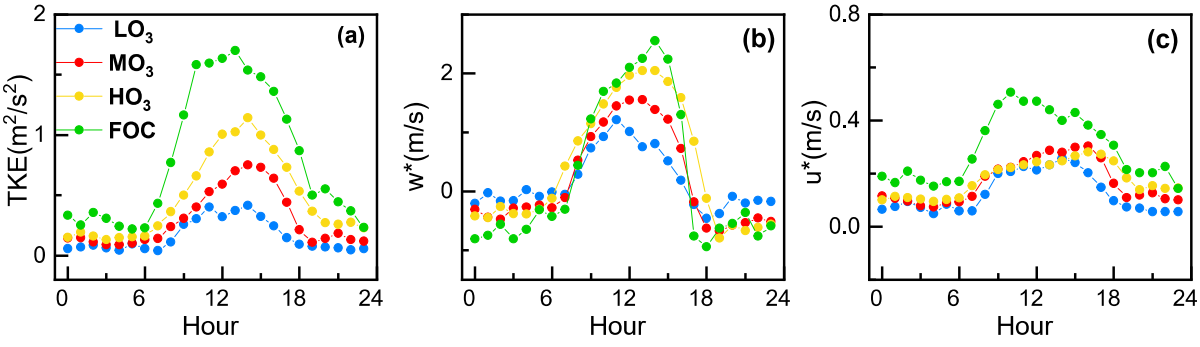

Fig. 2. Diurnal cycles of TKE (a), w* (b) and u* (c) under different environmental conditions. LO_3, MO_3, and HO_3 denote free convection days with $O_{3\text{-}8M}$ concentrations lower than 40 ppbv, 40–80 ppbv and greater than 80 ppbv, respectively, and FOC denotes forced convection days.

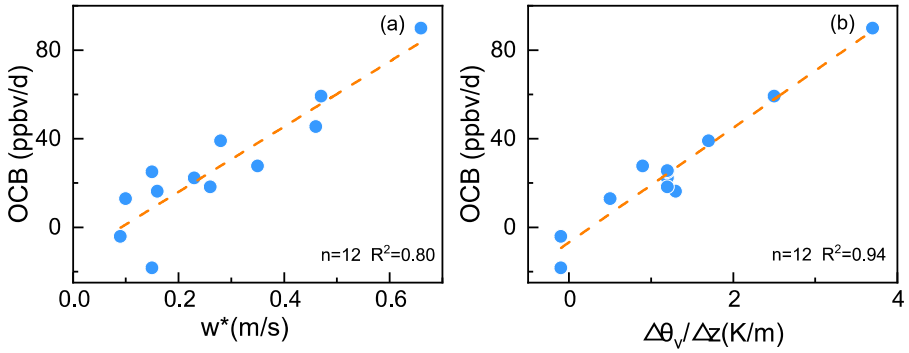

Fig. 4. Relationship between OCB and daily averaged w* (a) and OCB and the gradient of θ_v between 0 and 100 m in the afternoon (b). OCB denotes ozone chemical budget.

31.5–128.3 ppbv in the afternoon, and the ozone chemical budget was −18.3–89.9 ppbv/d. Afterwards, the relationship between the ozone chemical budget and free convection is analyzed. A significant positive correlation between ozone chemical budget and daily averaged w* was found, with R^2 values as high as 0.80 (Fig. 4a). Compared with the results using $O_{3\text{-}8M}$ and midday averaged ozone column concentrations (Fig. S6; $R^2 \approx 0.5$), this result features a significantly higher correlation coefficient. On the other hand, the θ_v gradient in the vertical direction in the afternoon can also characterize the intensity of free convection (Ellis et al., 2000). By calculating the θ_v gradient from 0 m to 100 m, it is found that the θ_v gradient is closely related to the ozone chemical budget, with an R^2 value as high as 0.94 (Fig. 4b). Therefore, by eliminating the contribution of ozone stored in the residual layer to ozone, the positive relationship between the ozone chemical budget and free convection intensity is fully confirmed.

4. Discussion

Generally, the lifetime of VOCs is longer than that of NOx. Due to the difference in the lifetimes of VOCs and NOx, the ratio of VOCs to NOx will change under different boundary layer conditions, which will affect ozone sensitivity. NO_2 and HCHO column concentrations observed by TROPOMI were used to analyze ozone sensitivity under different boundary layer conditions. With the deterioration of ozone pollution, the NO_2 concentration decreased significantly from 1.6×10^{16} to 8.3×10^{15} molc/cm^3 (Fig. 5a), but the HCHO concentration was approximately 9×10^{15} molc/cm^3 (Fig. 5b). This phenomenon led to an increase in the $HCHO/NO_2$ ratio with an increasing ozone concentration, indicating that ozone sensitivity evolved from VOC sensitivity to NOx sensitivity (Fig. 5c). Therefore, the free convection intensity drove the change in ozone sensitivity, which affects the occurrence and development of ozone pollution.

From the above analysis, under forced convection conditions, high BLH and high WS are beneficial for the dilution and diffusion of ozone and its precursors in the boundary layer. Compared with free convection conditions, a greater reduction in NO_2 and a constant HCHO induce an increase in the ratio of HCHO and NO_2 (Fig. 5), and ozone production is controlled by NOx (Fig. 6a). Under these conditions, low ozone production leads to ozone close to the background concentration, which is similar to previous research results (Minoura, 1999). However, stable atmospheric stratification does not lead to serious ozone pollution. In contrast, ozone pollution is aggravated under strong free convection conditions, which is contrary to most previous studies (Haman et al., 2014; Garrido-perez et al., 2019).

The main reason is that ozone is not a primary air pollutant but a product of secondary reactions. For primary air pollutants, the main sinks are dilution, diffusion, deposition and degradation by chemical reaction. With the increase in BLH, strong convection is conducive to the diffusion and deposition of air pollutants, so the primary pollutants are usually negatively correlated with the BLH (Tang et al., 2016). For the secondary air pollutant ozone, ozone mainly comes from the chemical reaction of NOx and VOCs. The near-surface layer emits a large amount of NOx, but these NOx mainly exist in the form of NO. Therefore, the near-surface ozone will react with NO to form NO_2, resulting in the chemical loss of ozone (Berkowitz et al., 2000). NO_2 generated by chemical reactions is transported to the upper boundary layer under the influence of turbulence, and then photolysis forms ozone in the upper boundary layer (Tang et al., 2017, 2021b). Strong turbulence also mixes the ozone generated in the upper boundary layer to the near-surface layer (Rappenglück et al., 2008), which makes up for the ozone lost due to the reaction with NO, thus characterizing the uniform ozone concentration at midday (Fig. 3b).

Therefore, strong free convection will lead to the transport of NO_2 generated near the ground to the upper boundary layer and will mix ozone from the upper boundary layer to the near ground, thus strengthening this photochemical process (Fig. 6b). In contrast, if the BLH is very low and the free convection is weak, a large amount of emitted NO will accumulate near the ground (Cazorla, 2016), which weakens the

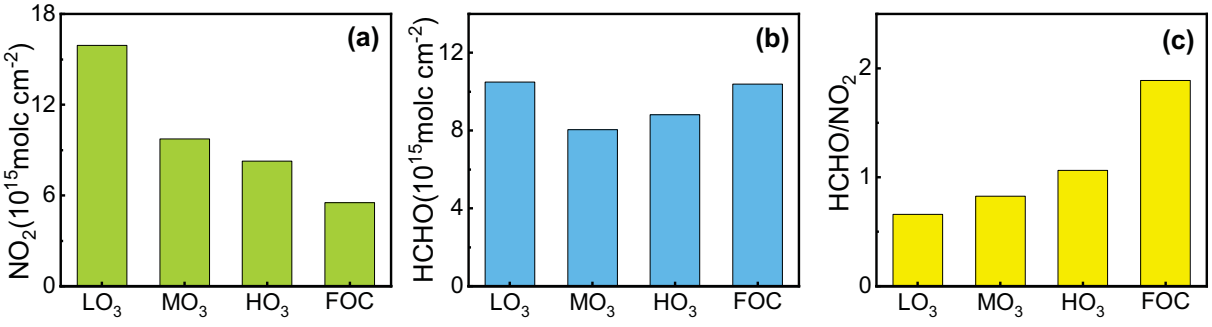

Fig. 5. Space-based NO_2 (a), HCHO (b) column concentrations and $HCHO/NO_2$ (c) observed by TROPOMI under different environmental conditions. LO_3, MO_3, and HO_3 denote free convection days with $O_{3\text{-}8M}$ concentrations lower than 40 ppbv, 40–80 ppbv and greater than 80 ppbv, respectively, and FOC denotes forced convection days.

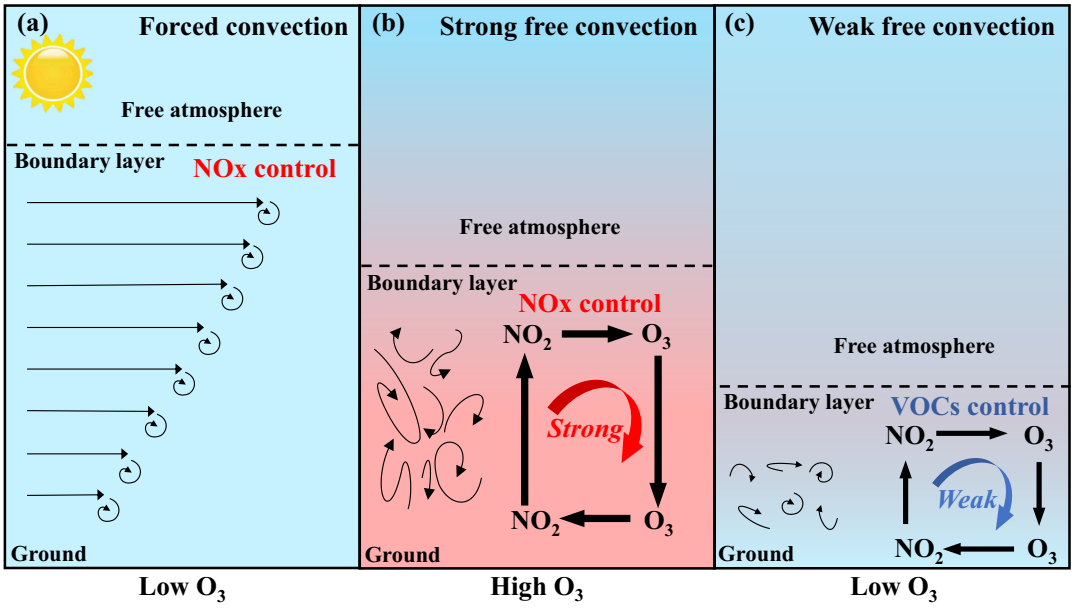

Fig. 6. Schematic diagram of the impact of forced convection (a), strong (b) and weak (c) free convection conditions on ozone pollution.

vertical physicochemical cycle and exhibits lower ozone in the lower boundary layer and high ozone in the high boundary layer (Fig. 3b). Therefore, weak free convection conditions induce weak ozone production (Fig. 6c).

5. Conclusions

To understand the impact of boundary layer meteorology on ozone pollution, two field observation experiments were carried out in summer in Shijiazhuang, the area with the most serious photochemical pollution on the North China Plain. Near-surface ozone and its corresponding meteorological and micrometeorological parameters were observed, and tethered balloon experiments were carried out simultaneously to obtain the vertical profiles of ozone in the morning and afternoon. After distinguishing the free and forced convection boundary layers using the vertical profiles of the atmospheric backscattering coefficient, three main conclusions were obtained.

(1). Under strong free convection conditions, intense radiation leads to increases in T, WS and BLH. Strong turbulence makes the physical and chemical cycle of ozone and its precursors vigorous between the lower and upper boundary layers, resulting in the deterioration of ozone pollution.
(2). Under weak free convection conditions, weak radiation leads to a decrease in T and BLH and an increase in RH. Weak turbulence weakens the physical and chemical cycle of ozone and its precursors between the lower and upper boundary layers, causing more ozone titrates with freshly emitted NO.
(3). Under forced convection conditions, intense radiation makes T rise, RH decrease, and WS and BLH extremely high. The strong diffusion ability leads to a sharp decrease in the concentration of ozone and its precursors, and the concentration of ozone is close to the background concentration.

In summary, although the BLH cannot be used as an index to judge ozone pollution directly, it can be used as a reliable index to judge ozone pollution after excluding days with forced convection. This study clarified the impact of free convection on ozone concentration and its sensitivity and provided scientific support for ozone pollution prevention and early warning.

Data availability

All data generated or analyzed during this study are included in this published article and are available from the authors upon reasonable request.

CRediT authorship contribution statement

Guiqian Tang: Formal analysis, Methodology, Data curation, Writing – original draft, Conceptualization, Supervision, Funding acquisition. **Yuting Liu:** Visualization, Writing – review & editing. **Xiao Huang:** Investigation. **Yinghong Wang:** Methodology, Investigation. **Bo Hu:** Investigation, Writing – review & editing. **Yucui Zhang:** Investigation. **Tao Song:** Writing – review & editing. **Li Xiaolan:** Writing – review & editing. **Shuang Wu:** Investigation, Visualization. **Qihua Li:** Investigation. **Yanyu Kang:** Investigation. **Zhenyu Zhu:** Investigation. **Meng Wang:** Investigation. **Yiming Wang:** Visualization. **Tingting Li:** Writing – review & editing. **Xin Li:** Writing – review & editing. **Yuesi Wang:** Project administration, Funding acquisition.

Declaration of competing interest

The authors declare that they have no known competing financial interests or personal relationships that could have appeared to influence the work reported in this paper.

Acknowledgments

This work was supported by the National Key R&D Program of China (No. 2017YFC0210000), the National Natural Science Foundation of China (Nos. 41705113, 41877312), the National Research Program for Key Issues in Air Pollution Control (No. DGQQ202004), and the Beijing Major Science and Technology Project (No. Z181100005418014).

Appendix A. Supplementary data

Supplementary data to this article can be found online at https://doi.org/10.1016/j.scitotenv.2021.147740.

References

Athanassiadis, G., Rao, S., Ku, J., Clark, R., 2002. Boundary layer evolution and its influence on ground-level ozone concentrations, environ. Fluid Mech. 2, 339–357.

Banta, R., Senff, C., Alvarez, R., Langford, A., Parrish, D., Trainer, M., Darby, L., Hardesty, R., Lambeth, B., Neuman, J., Angevine, W., Nielsen-Gammon, J., Sandberg, S., White, A., 2011. Dependence of daily peak O_3 concentrations near Houston, Texas on environmental factors: wind speed, temperature, and boundary-layer depth, Atmos. Environ. 45, 162–173.

Banta, R., Senff, C., White, A., Trainer, M., McNider, R., Valente, R., Mayor, S., Alvarez, R., Hardesty, R., Parrish, D., Fehsenfeld, F., 1998. Daytime buildup and nighttime transport of urban ozone in the boundary layer during a stagnation episode. J. Geophys. Res. Atmos. 103, 22519–22544.

Berkowitz, C., Fast, J., Easter, R., 2000. Boundary layer vertical exchange processes and the mass budget of ozone: observations and model results. J. Geophys. Res. Atmos. 105, 14789–14805.

Cazorla, M., 2016. Air quality over a populated Andean region: insights from measurements of ozone, NO, and boundary layer depths, Atmos. Pollut. Res. 7, 66–74.

Chameides, W., Fehsenfeld, F., Rodgers, M., Cardelino, C., Martinez, J., Parrish, D., Lonneman, W., Lawson, D., Rasmussen, R., Zimmerman, P., Greenberg, J., Middleton, P., Wang, T., 1992. Ozone precursor relationships in the ambient atmosphere. J. Geophys. Res. Atmos. 97, 6037–6055.

Ellis, A., Hildebrandt, M., Thomas, W., Fernando, H., 2000. Analysis of the climatic mechanisms contributing to the summertime transport of lower atmospheric ozone across metropolitan Phoenix, Arizona, USA. Clim. Res. 15, 13–31.

Garrido-perez, J., Ordóñez, C., García-Herrera, R., Schnell, J., 2019. The differing impact of air stagnation on summer ozone across Europe. Atmos. Environ. 219, 117062.

Haman, C., Couzo, E., Flynn, J., Vizuete, W., Heffron, B., Lefer, B., 2014. Relationship between boundary layer heights and growth rates with ground-level ozone in Houston, Texas. J. Geophys. Res. Atmos. 119, 6230–6245.

Hidy, 2000. Ozone process insights from field experiments part I: overview. Atmos. Environ. 34, 2001–2022.

Hu, B., Wang, Y., Liu, G., 2010. Properties of ultraviolet radiation and the relationship between ultraviolet radiation and aerosol optical depth in China. Atmos. Res. 97, 297–308.

Jenkin, M., Clemitshaw, K., 2000. Ozone and other secondary photochemical pollutants: chemical processes governing their formation in the planetary boundary layer. Atmos. Environ. 34, 2499–2527.

Minoura, H., 1999. Some characteristics of surface ozone concentration observed in an urban atmosphere. Atmos. Res. 51, 153–169.

Olszyna, K., Luria, M., Meagher, J., 1997. The correlation of temperature and rural ozone levels in southeastern U.S.A. Atmos. Environ. 31, 3011–3022.

Rappenglück, B., Perna, R., Zhong, S., Morris, G., 2008. An analysis of the vertical structure of the atmosphere and the upper-level meteorology and their impact on surface ozone levels in Houston, Texas. J. Geophys. Res. Atmos. 113, D17315.

Seinfeld, J.H., Pandis, S.N., 1998. Atmospheric Chemistry and Physics, from Air Pollution to Climate Changes. 1326. Wiley, New York, USA.

Solomon, P., Cowling, E., Hidy, G., Furiness, C., 2000. Comparison of scientific findings from major ozone field studies in North America and Europe. Atmos. Environ. 34, 1885–1920.

Stull, R., An Introduction to Boundary Layer Meteorology, Kluwer Academic Publisher, Norwell, USA, 669pp, 1988.

Tang, G., Li, X., Wang, Y., Xin, J., Ren, X., 2009. Surface ozone trend details and interpretations in Beijing, 2001–2006. Atmos. Chem. Phys. 9, 8813–8823. https://doi.org/10.5194/acp-9-8813-2009.

Tang, G., Wang, Y., Li, X., Ji, D., Hsu, S., Gao, X., 2012. Spatial-temporal variations in surface ozone in northern China as observed during 2009–2010 and possible implications for future air quality control strategies. Atmos. Chem. Phys. 12, 2757–2776. https://doi.org/10.5194/acp-12-2757-2012.

Tang, G., Zhu, X., Hu, B., Xin, J., Wang, L., Münkel, C., Mao, G., Wang, Y., 2015. Impact of emission controls on air quality in Beijing during APEC 2014: lidar ceilometer observations. Atmos. Chem. Phys. 15, 12667–12680. https://doi.org/10.5194/acp-15-12667-2015.

Tang, G., Zhang, J., Zhu, X., Song, T., Münkel, C., Hu, B., Schäfer, K., Liu, Z., Zhang, J., Wang, L., Xin, J., Suppan, P., Wang, Y., 2016. Mixing layer height and its implications for air pollution over Beijing, China. Atmos. Chem. Phys. 16, 2459–2475. https://doi.org/10.5194/acp-16-2459-2016.

Tang, G., Zhu, X., Xin, J., Hu, B., Song, T., Sun, Y., Zhang, J., Wang, L., Cheng, M., Chao, N., Kong, L., Li, X., Wang, Y., 2017. Modelling study of boundary-layer ozone over northern China - part I: ozone budget in summer. Atmos. Res. 187, 128–137. https://doi.org/10.1016/j.atmosres.2016.10.017.

Tang, G., Wang, Y., Liu, Y., Wu, S., Huang, X., Yang, Y., Wang, Y., Ma, J., Bao, X., Liu, Z., Ji, D., Li, T., Li, X. and Wang, Y., Low particulate nitrate in the residual layer in autumn over the North China Plain. Sci. Total Environ., 782, 146845, doi:https://doi.org/10.1016/j.scitotenv.2021.146845, 2021a.

Tang, G., Liu, Y., Zhang, J., Liu, B., Li, Q., Sun, J., Wang, Y., Xuan, Y., Li, Y., Pan, J., Li, X., Wang, Y., 2021b. Bypassing the NOx titration trap in ozone pollution control in Beijing. Atmos. Res. 249, 150333. https://doi.org/10.1016/j.atmosres.2020.105333.

Tong, N., Leung, D., Liu, C., 2011. A review on ozone evolution and its relationship with boundary layer characteristics in urban environments. Waste Air Soil Pollut. 214, 13–36.

Vukovich, F., 1994. Boundary layer ozone variations in the eastern United States and their association with meteorological variations: long-term variations. J. Geophys. Res. Atmos. 99, 16830–16839.

Wu, S., Tang, G., Wang, Y., Yang, Y., Yao, D., Zhao, W., Gao, W., Sun, J., Wang, Y., 2020. Vertically decreased VOC concentration and reactivity in the planetary boundary layer in winter over the North China Plain. Atmos. Res. 240, 104930.

Wu, S., Tang, G., Wang, Y., Mai, R., Yao, D., Kang, Y., Wang, Q., Wang, Y., 2021. Vertical evolution of boundary layer VOCs in summer over the North China plain and differences between winter and summer. Adv. Atmos. Sci. https://doi.org/10.1007/s00376-020-0254-9.

Zhang, Y., Lei, H., Zhao, W., Shen, Y., Xiao, D., 2018. Comparison of the water budget for the typical cropland and pear orchard ecosystems in the North China Plain. Agric. Water Manag. 198, 53–64.

Zhang, C., Liu, C., Hu, Q., Cai, Z., Su, W., Xia, C., Zhu, Y., Wang, S., Liu, J., 2019. Satellite UV-Vis spectroscopy: implications for air quality trends and their driving forces in China during 2005–2017. Light: Sci. Applic. 8 (1), 1–12.

Zhao, W., Tang, G., Yu, H., Yang, Y., Wang, Y., Wang, L., An, J., Gao, W., Hu, B., Cheng, M., An, X., Li, X., Wang, Y., 2019. Evolution of boundary layer ozone in Shijiazhuang, a suburban site on the North China Plain. J. Environ. Sci. 83, 152–160. https://doi.org/10.1016/j.jes.2019.02.016.

Zhu, X., Ma, Z., Qiu, Y., Liu, H., Liu, Q., Yin, X., 2020. An evaluation of interaction of morning residual layer ozone and mixing layer ozone in rural areas of the North China Plain. Atmos. Res. 236, 104788.